Weyl- and Dirac-fermions in a three bands model

Ludovic Le Laurent

June 20, 2017

Tutor : Mark-Oliver Goerbig

Remerciements

Je tiens à remercier toute l'équipe du groupe théorique du LPS pour son accueil et sa bonne humeur : Sergueï Tchoumakov pour son encadrement et ses blagues douteuses, Pierre Bruneel qui a partagé mon bureau, Frédéric Combes pour les pauses de 16h, ainsi que Marc Gabay, Manali Vivek et tous les autres que j'oublie pour les discussions et échanges intéressants que nous avons eus.
Je souhaite remercier tout particulièrement Mark-Oliver Goerbig, qui m'a accepté en tant que stagiaire et qui a su m'aiguiller dans ce projet, avec qui je souhaitais tout particulièrement poursuivre en thèse : ne serait-ce que pour sa bonne humeur et ses amandes grillées.

Abstract

Particles coupled to a lattice give birth to the so-called quasiparticles. These last ones are actually described by their band spectrum : such as in the case of Dirac fermions. However, the Hamiltonian provides further information, that can be found in the wavefunction characterized by topological quantities. These are the Berry phase, Berry curvature and Chern number, which appear often while symmetries are broken by a gap opening between bands.
In this report I exemplify these concepts in the paradigmatic twodimensional honeycomb structure (graphene), with the Semenoff and Haldane models, and the observation of topological phase transitions well defined between insulating states. The ultimate aim is to study the impact of a third band in a similar spectrum as that of graphene, as well as three-dimensionnal materials.
In order to approach this problem, we make use, here, of a tight-binding model on the two dimensions Kagomé lattice, that hosts Dirac-like bands as well as a flat one and then deform the parameters to introduce explicite time-reversal and inversion symmetry breaking terms.

Résumé

Les particules couplées à un réseau donnent naissance à ce qu'on appelle quasiparticules. Elles sont en général décrites par leur spectre en bande : tel est le case des fermions de Dirac. Cependant, l'hamiltonien comporte d'autres informations, que l'on trouve dans la fonction d'onde, caractérisée par des quantités topologique, telles que les phase Berry, courbure de Berry et nombre de Chern, qui ne s'expriment souvent que lors de brisure de symétrie par l'ouverture d'un gap entre les bandes.
Dans ce rapport, j'illustrerai ces concepts avec la très représentative structure bidimensionnelle en nid d'abeille (graphène), avec les modèles de Semenoff et Haldane, avec l'observation de transitions de phase topologique bien définies entre des états isolants. Le sujet de la thèse suivante est d'étudier l'impact d'une troisième bande dans un spectre semblable à celui du graphène, comme c'est le cas dans des matériaux tridimensionnels.
Afin d'étudier ce problème, on utilisera ici un modèle de liaisons fortes sur le réseau bidimensionnel de Kagomé, dont la spectre est composé de deux bandes de type Dirac et d'une troisième plate. On déformera ensuite ce réseau pour introduire explicitement des termes de brisure de symétrie par renversement du temps et par inversion.

Contents

1 Introduction

A major field of Condensed matter theory is the study of particles in a lattice, mostly in the form of site band spectrum, whose recently, topological aspect have gained interest. These aspects are encoded in the wavefunctions of lattice electrons rather than in its spectrum.
Indeed, we know that Dirac fermions are characterized by a linear dispersion, but a linear dispersion is a characteristic of Weyl fermions too, and thus not a distinctive feature. These novel fermions are examples of the topological role encoded in the wavefunction.
How can we characterize the wavefunction ?

A good way to study topology of electronic bands, is the Berry phase, which is in fact the phase earned by the evolution of a parameter as the lattice momentum $\vec{k}$ around a closed path on the Bloch sphere for example. The Berry phase is defined in terms of the Berry connexion, which is in fact the integrand along this closed path, and acts as a "vector potential" in reciprocal space. By the same process as in electromagnetism, we can define a "magnetic field", the Berry curvature which is the curl of the "vector potential". These two concepts translate in fact how the Bloch sphere is covered by the wavefunction, and can be computed only for non degenerated states, i.e. isolated bands. A simplest way to show this, is to use the winding number or the Chern number, which are in fact the integration of Berry curvature along the first Brillouin zone, which describes the winding number around a singularity on the Bloch sphere. These concepts are topological ones, since they teach us about the topology of the Bloch sphere. Such singularities are seen with the opening of a gap, which can yield topological phase transitions, between two insulating states.
Moreover, the results in two bands models are known, and we would like to see how a third band could make evolve the topological aspects of a system with linear dispersion.

What is the influence of a third band in a linear dispersion system ?

In a first part, I study the case of two-band model with the honeycomb structure, to get familiarized with these new concepts. We will also see the different manners to open a gap, and move bands.
In the second part of this report, I will talk about the three-band model in two dimensions for simplicity, and the computation of the Chern numbers in such systems, to see the contribution in Chern numbers and winding numbers of the third band. The computation of these numbers could make place to the rising of new phase transitions, or new quasiparticles.
During this report, I will only present 2D systems for conceptual simplicity. The generalisation to 3D systems is the long term goal of this study which I prospect to pursue within a PhD thesis in the theory group at Laboratoire de Physique des Solides.

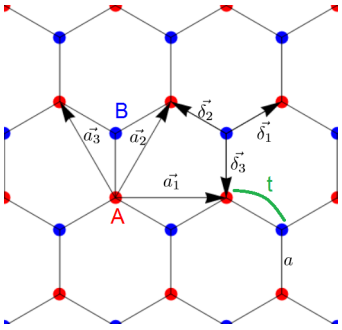

Figure 1: Graphene lattice, defined by vectors $\vec{a_1}, \vec{a_2}, \vec{\delta_1}, \vec{\delta_2}$ and $\vec{\delta_3}$.

2 Two-band model

2.1 Graphene and insulators

2.1.1 Graphene

Graphene is a single one-atom-thick layer of graphite, i.e. crystalline carbon, where the carbon atoms are arranged in a 2D bidimensional honeycomb lattice with a nearest-neighbour distance $a = 0.142$nm (fig.1). This is not a Bravais lattice, but composed of two triangular Bravais sublattices called A and B here. The sublattice A has the following basis (with the lattice parameter set to one) : $\vec{a_1} = \sqrt{3}\vec{e_x}$, $\vec{a_2} = \frac{\sqrt{3}}{2}(\vec{e_x} + \sqrt{3}\vec{e_y})$ and $\vec{a_3} = \vec{a_2} - \vec{a_1} = \frac{\sqrt{3}}{2}(-\vec{e_x} + \sqrt{3}\vec{e_y})$.
The two sublattices are connected by the following set of vectors : $\vec{\delta_1} = \frac{1}{2}(-\sqrt{3}\vec{e_x} + \vec{e_y})$, $\vec{\delta_2} = \frac{1}{2}(\sqrt{3}\vec{e_x} + \vec{e_y})$ and $\vec{\delta_3} = -\vec{e_y}$.
The reciprocal lattice is defined as follows : $\vec{a_i^*}.\vec{a_j} = 2\pi\delta_{ij}$, and thus :
$\vec{a_1^*} = \frac{2\pi}{\sqrt{3}}(\vec{e_x} - \frac{1}{\sqrt{3}}\vec{e_y})$ and $\vec{a_2^*} = \frac{4\pi}{3}\vec{e_y}$. Since the reciprocal lattice keeps the symmetries of the direct one, the first Brillouin zone has the shape of a hexagon.

In order to compute the Hamiltonian of such a structure, we use the tight-binding approximation, where we consider a non-zero hopping term $t \simeq 3$ eV (for graphene) only between the nearest neighbours : $H = t \sum_{<ij>} c_i^\dagger c_j + h.c.$, where $c_i^{(\dagger)}$ destroys (creates) an electron on the site i. In order to apply Bloch theorem, it is more convenient to use the notation of the sublattice A : $H = t \sum_{\vec{r_A}} \sum_{\alpha} c_B^\dagger(\vec{r_A} + \vec{\delta_\alpha}) c_A(\vec{r_A}) + h.c.$, where $\alpha = 1, 2, 3$.
The electron operator can then be Fourier-transformed : $c_A(\vec{r_i}) = \frac{1}{\sqrt{N}} \sum_k e^{-i\vec{k}.\vec{r_i}} c_A(\vec{k})$, and identically for B, such that the Hamiltonian becomes :

$$H = t \sum_{\vec{k}} \Big[\gamma(\vec{k}) c_B^\dagger(\vec{k}) c_A(\vec{k}) + h.c. \Big],$$

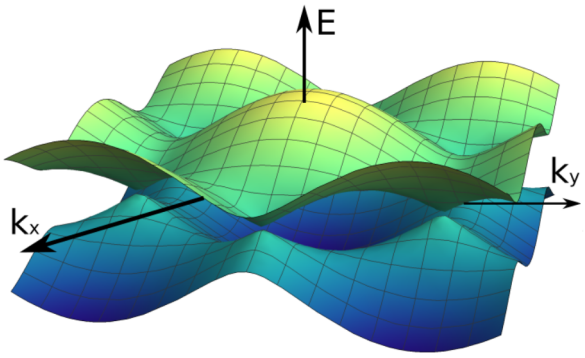

Figure 2: Graphene spectrum with contact points at $\pm\vec{K}$.

setting $\gamma(\vec{k}) = \sum_{\alpha} e^{i\vec{\delta_\alpha}.\vec{k}}$, and using $\sum_{\vec{r_i}} e^{-i\vec{k}.\vec{r_i}} = N\delta_{\vec{k},\vec{0}}$.
We can express this Hamiltonian in matrix form :

$$H^0_{\vec{k}} = \begin{pmatrix} 0 & t\gamma^* \\ t\gamma & 0 \end{pmatrix}, \tag{1}$$

whose spectrum $\mathrm{E} = \pm t|\gamma|$ is represented in figure 2, and associated eigenstates read :

$$|\psi^{\pm}\rangle = \frac{1}{\sqrt{2}} \begin{pmatrix} 1 \\ \pm\frac{\gamma}{|\gamma|} \end{pmatrix} = \frac{1}{\sqrt{2}} \begin{pmatrix} 1 \\ \pm e^{i\theta} \end{pmatrix}, \tag{2}$$

with $\theta = \arctan(\frac{\Im(\gamma)}{\Re(\gamma)})$, defined on the Bloch sphere. We can thus associate a polarization to these states on the Bloch sphere. The states are characterized by the $\vec{k}$-dependent relative phase between the two components, while their relative weight $(\frac{1}{2})$ remains unchanged. The polarization thus evolves on the equator of the Bloch sphere (fig.3).
The first Brillouin zone corresponds to the set of inequivalent points in the reciprocal space. We see that the two bands, conduction (up) and valence (down), are in contact at some points (fig.2). Since there are as many conduction electrons as lattice sites, each of which can host two particles (spin up and down) according to the Pauli principle, the bands shown in figure 2 are half filled, such that the Fermi energy is situated in the band contact points $\gamma(\pm\vec{K}) = 0$. One finds the two inequivalents Dirac points : $\pm\vec{K} = \pm\frac{4\pi}{3\sqrt{3}}\vec{e_x}$, the others four corners are found by primitive translation on the reciprocal lattice.
In fact, since the contact point between the two bands corresponds to the Fermi energy, it means that the upper band is totally empty whereas the lower one is totally filled. Hence, because of the Pauli principle, the dynamics of the system is near these inequivalent points $\pm\vec{K}$. Since we study this material at ambiant temperature, the electrons are in a range of energy around $t \simeq 10^{-2}$ eV, the saddle point of the spectrum is around $t \simeq 3$ eV. So we can make a study at low energy by a linearization around these Dirac points.

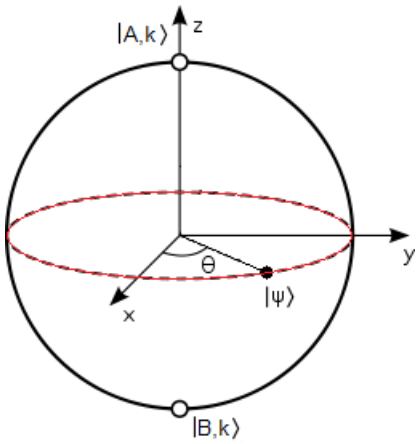

Figure 3: Bloch sphere representing the eigenstates, for the graphene they evolve on the equator, in red here.

Low energy study

In order to obtain the low-energy model, we expand the tight-binding Hamiltonian around the band contacts $\xi\vec{K}$, $\vec{k} = \xi\vec{K} + \vec{q}$, where $\xi = \pm 1$, denotes the Dirac point. Indeed, $E \ll t$, is equivalent to $qa \ll 1$, by linearization. Using $\gamma(\vec{k}) = 1 + e^{i\vec{a_2}.\vec{k}} + e^{i\vec{a_3}.\vec{k}}$,
we recognize the unity roots : $e^{i\xi\vec{K}.\vec{a_2}} = j^{\xi}$ and $e^{i\xi\vec{K}.\vec{a_3}} = j^{-\xi}$. And thus, $\gamma(\vec{k}) = 1 + j^{\xi}e^{i\xi\vec{q}.\vec{a_2}} + j^{-\xi}e^{i\xi\vec{q}.\vec{a_3}}$, where $j = e^{\frac{2i\pi}{3}}$.
At first order in q, one finds,
$\gamma(\vec{k}) = 1 + j^{\xi}(1 + i\xi\vec{q}.\vec{a_2}) + j^{-\xi}(1 + i\xi\vec{K}.\vec{a_3}) = i\vec{q}(j^{\xi}\vec{a_2} + j^{-\xi}\vec{a_3}) = -\frac{3}{2}(\xi q_x + iq_y)$, which we can write $\hbar v_F(\xi q_x + iq_y)$, where $v_F = \frac{t}{\hbar}|\partial_{\vec{k}}\gamma|_{\vec{K}} = \frac{3ta}{2\hbar}$ is the Fermi velocity.
In matrix form, the Hamiltonian becomes :

$$H = \hbar v_F \begin{pmatrix} 0 & \xi q_x - iq_y \\ \xi q_x + iq_y & 0 \end{pmatrix}, \tag{3}$$

which can be written in the basis of Pauli matrices (see appendix), $H = \hbar v_F(q_x\sigma_x + \xi q_y\sigma_y)$.
One thus obtains the spectrum $E_{\vec{q}} = \pm\hbar v_F\sqrt{q_x^2 + q_y^2}$, which coincides with that of ultrarelativistic (massless) bidimensionnal Dirac fermions. Indeed, we obtain a linear dispersion in Dirac cones (fig.4).

2.1.2 How to obtain a topological insulator ?

An important point here is the following : we have singularities in the wavefunction phase at $\vec{k} = \vec{K}$, which can give some useful information to qualify our quasiparticle. Such singularities have important contribution in the Berry connexion, or Berry curvature (see appendix) :

$$\vec{Ak} = i\langle\psi(\vec{k})|\nabla_{\vec{k}}\psi(\vec{k})\rangle, \tag{4}$$

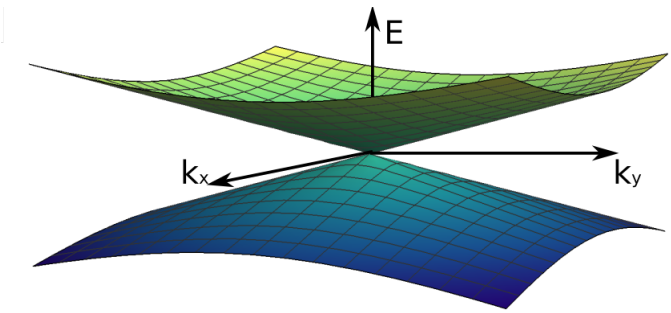

Figure 4: Linear dispersion as Dirac cones.

$$\vec{\Omega k} = \nabla_{\vec{k}} \wedge \vec{A k}. \tag{5}$$

The integration of Eq.(5) over the entire first Brillouin zone gives an integer, the Chern number. This one permits to quantify the edge states, e.g. the quantum Hall effect. Here, it acts as an order parameter, qualifying a topological phase : it is a topological number.
However, there is a problem : $\vec{Ak}$ is not defined at the band contact points, where the bands are degenerate. A way to lift this degeneracy is to open a gap between bands, which constrains the Chern number, and gives birth to topological phase transitions. There are several ways to make an insulator, such as the Semenoff, Haldane and Kane-Mele models, which I will briefly discuss in the following paragraphs.

Semenoff model : example of the boron nitride

We could open a gap giving a mass to the fermions, indeed in the Dirac equation (see appendix) $E^2 = m^2 v_F^4 + \hbar^2 \vec{k}^2 v_F^2$, m$\neq$ 0 implies a non zero energy at band contact points $\xi \vec{K}$.
This can be done adding a term $\delta\sigma_z$ to the Hamiltonian (1) of the graphene. In fact, this is the case of boron nitride, which has the same structure of the graphene, but opposite potentials on the site A and B.
The eigenvalues of a such Hamiltonian are : $E = \pm t\sqrt{\gamma^2 + \delta^2}$. Hence, we have a gap of 2δ between the conduction and valence bands. Moreover, the presence of this mass implies a broken inversion symmetry, such that one no longer has : $PHP^{-1} = -H$. The eigenstates of the system are :

$$|\phi^{\pm}\rangle = \frac{1}{\sqrt{2}} \begin{pmatrix} \sqrt{1 + \frac{\pm\delta}{\sqrt{|\gamma|^2+\delta^2}}} \\ \pm\sqrt{1 - \frac{\pm\delta}{\sqrt{|\gamma|^2+\delta^2}}} e^{i\theta} \end{pmatrix}. \tag{6}$$

Similarly to graphene, the non-energy model can be obtained and reads :

$$H = \begin{pmatrix} mv_F^2 & \hbar v_F(\xi k_x - i k_y) \\ \hbar v_F(\xi k_x + i k_y) & -mv_F^2 \end{pmatrix}, \tag{7}$$

where $mv_F^2 = \delta$. The eigenstates evolve similarly on the Bloch sphere, but no longer on the equator but at a latitude determined by its energy.

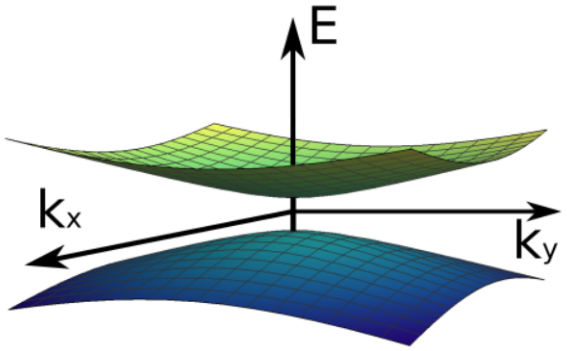

Figure 5: The Semenoff spectrum at low energy

Haldane model

Another manner to have an insulating state avoiding the breaking of parity invariance is Haldane's idea. In addition to the first nearest neighbours, we consider also the second-nearest hopping, i.e. between two A/B sites of the form : $t'e^{i\phi}$ between A sites, and $t'e^{-i\phi}$ between B sites, such that the total flux in the honeycomb is zero (fig.6). The Hamiltonian of a such system in matrix form is written :

$$H = \begin{pmatrix} t_{\vec{k}}^{AA} & t\gamma_{\vec{k}}^{*} \\ t\gamma_{\vec{k}} & t_{\vec{k}}^{BB} \end{pmatrix}, \tag{8}$$

whose the spectrum is :

$$\epsilon_{\vec{k}} = \frac{t_{\vec{k}}^{AA} + t_{\vec{k}}^{BB}}{2} \pm \sqrt{(\frac{t_{\vec{k}}^{AA} - t_{\vec{k}}^{BB}}{2})^2 + t^2|\gamma_{\vec{k}}|^2}, \tag{9}$$

where $\pm$ denotes the band, - for the valence band, + for the conduction.
We can write for A sites :
$t_{\vec{k}}^{AA} = 2t\left[\cos\phi(\cos\vec{k}.\vec{a_1} + \cos\vec{k}.\vec{a_2} + \cos\vec{k}.\vec{a_3}) - \sin\phi(\sin\vec{k}.\vec{a_1} + \sin\vec{k}.\vec{a_2} + \sin\vec{k}.\vec{a_3})\right]$,
and for B sites, the same expression but with $-\phi$. Using Eq.(9) :

$$\epsilon_{\vec{k},\phi} = 2t\cos\phi\sum_{i=1}^{3}\cos\vec{k}.\vec{a_i} \pm \sqrt{4t'^2\sin^2\phi\sum_{i=1}^{3}\sin\vec{k}.\vec{a_i} + t^2|\gamma_{\vec{k}}|} \tag{10}$$

There is a gap modulated by ϕ, indeed if $\phi = 0$ we find the result without dephasing and so a closure of the gap, if $\phi = 0[\pi]$ we have the time reversal symmetry, for the others values, this symmetry is broken. In fact, as in the Semenoff model, we can write the Haldane term in the Hamiltonian thanks to the σ_z matrix (see appendix) :

$$H_{haldane}(\vec{k},\phi) = 2t'\cos\phi\sum_i\cos\vec{k}.\vec{a_i}\mathbb{1} + 2t'\sin\phi\sum_i\sin\vec{k}.\vec{a_i}\sigma_z. \tag{11}$$

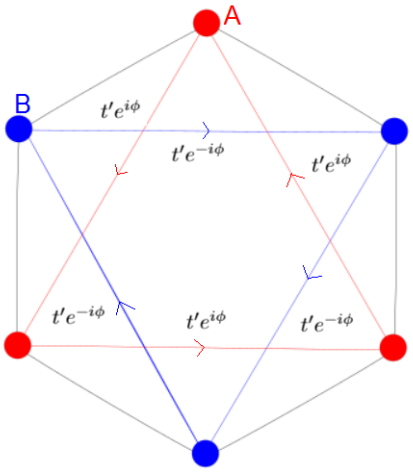

Figure 6: Second nearest neighbour interaction as in Haldane case.

At low energy, i.e. around the Dirac points (we assume also here $E \ll t'$),

$$H(\vec{k},\phi) = H^0_{\vec{k}} + H_{haldane}(\vec{k},\phi) = -3t'\cos\phi\mathbb{1} - \xi 3\sqrt{3}t'\sin\phi\sigma_z + H^0_{\vec{k}}, \tag{12}$$

which gives a gap of $6\sqrt{3}t'\sin\phi$ between the two bands.
I have computed the associated eigenstates, which evolve as same as the preceeding cases on the Bloch sphere, according to their energy (fig.3) :

$$|\phi^{\pm}\rangle = \frac{1}{\sqrt{2}}\begin{pmatrix} \sqrt{1+\frac{\pm\xi 3\sqrt{3}t'\sin\phi}{\sqrt{|\gamma|^2+27t'^2\sin^2\phi}}} \\ \pm\sqrt{1-\frac{\pm\xi 3\sqrt{3}t'\sin\phi}{\sqrt{|\gamma|^2+27t'^2\sin^2\phi}}}e^{i\theta} \end{pmatrix}. \tag{13}$$

Kane-Mele model

The Kane-Mele model is similar to Haldane's : indeed we consider second nearest neighbours hopping with a dephasing ϕ, but we add here spin considerations. In fact, for spin up, we have the Haldane model between sites A, respectively B, and for spin down, we have the complex conjugate of the Haldane model between sites A, respectively B (fig.7). We have now a 4x4 matrix, composed of 2 diagonal blocks, one for spin up, the second for spin down which are Haldane-like. The up-like one is exactly the Haldane Hamiltonian, the down-like one is its complex conjugate.

$$H_{Kane-Mele} = \begin{pmatrix} H_{Haldane}(\vec{k},\phi) & 0 \\ 0 & H_{Haldane}(\vec{k},-\phi) \end{pmatrix}. \tag{14}$$

Thus, we obtain two sets of twofold-degenerated states, because there is still the spin degeneracy.

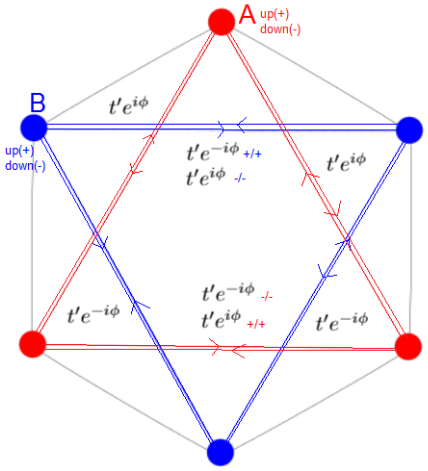

Figure 7: Kane-Mele model.

2.2 Topological phase transition

It is important to see that we can hybridize the preceeding models. For the following study, we consider the Haldane model with a Semenoff mass. The Haldane-Semenoff Hamiltonian is written :

$$H_{diag} = 2t' \cos\phi \sum_i \cos \vec{k}.\vec{b_i} \mathbb{1} + 2t' sin\phi \sum_i \sin \vec{k}.\vec{b_i} \sigma_z + \delta\sigma_z. \tag{15}$$

At low energy, i.e. near the Dirac points for the same energy considerations as before, $\vec{k} = \xi\vec{K} + \vec{q}$,

$$H = -3t' \cos\phi \mathbb{1} - \xi 3\sqrt{3} t' \sin\phi \sigma_z + \delta\sigma_z. \tag{16}$$

The gap comes from the terms in σ_z, so in the total Hamiltonian we have a term $(\delta - \xi 3\sqrt{3}\sin\phi)\sigma_z$, which can be zero in some cases, and thus, gives two kinds of insulators : Haldane-like governed principally by a broken time-reversal symmetry, and Semenoff-like with a stronger inversion symmetry breaking gap. The two phases are distinct topological phases : while the Semenoff-like is a trivial insulator, with zero Chern number, the Haldane-like phase is a topological insulator with a ± 1 Chern number. A phase transition between the two is accompanied by a gapless (massless) Dirac phase, where the gap vanishes at one of the Dirac points. Indeed, this can occur due to a broken time-reversal symmetry $\epsilon_{\vec{k}} \neq \epsilon_{-\vec{k}}$. Here, the phase transition occurs when varying ϕ and δ (fig.8) :
If $\delta = 3\sqrt{3}|\sin\phi|$, we find massless graphene only for one of the two Dirac cones, constrained by the Chern number.

Characterization with topological numbers

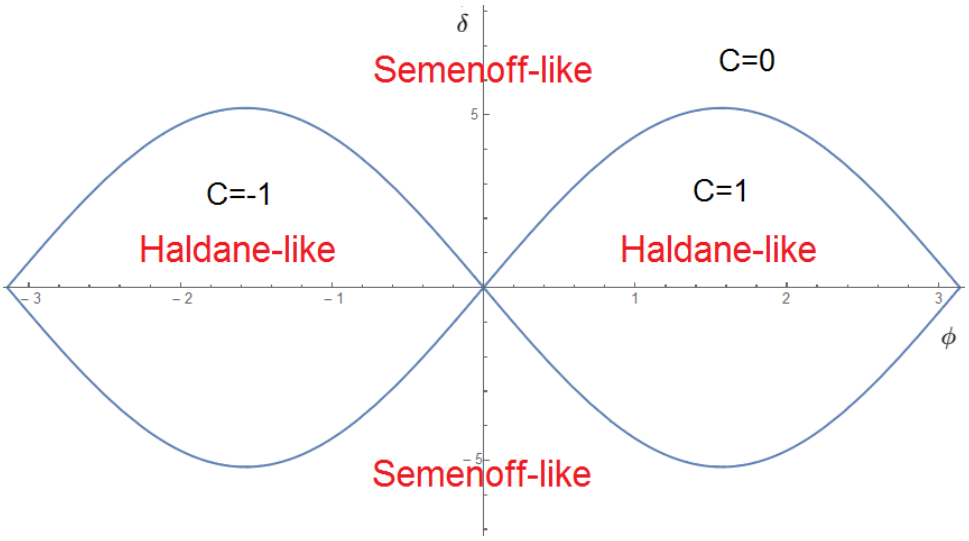

Figure 8: Topological phase diagram transition.

In the preceeding example, we can define as explained in the appendix : $h_x = v_F k_x$, $h_y = v_F k_y$ and $h_z = (\delta - 3\sqrt{3}\xi t' \sin\phi)$.
We compute the variation of Chern number, according to the appendix, in each phase, only around the Dirac points, which is sufficient instead of the continuous study on all the first Brillouin zone because the Berry curvature is zero everywhere except in the vicinity of these points :

- in the Semenoff phase, i.e. $\delta > 3\sqrt{3}|\sin\phi|$, $C_\xi^- = \xi\frac{1}{2}$, is the contribution of one of the Dirac points, denoted by ξ, to the Chern number, or winding number, thus we have $n_w = 0$.

- in the Haldane phase, i.e. $\delta < 3\sqrt{3}|\sin\phi|$, $C_\xi^- = \frac{1}{2}\frac{\sin\phi}{|\sin\phi|}$, thus $n_w = \frac{\sin\phi}{|\sin\phi|}$: if $\phi \in]0,\pi[$, $n_w = 1$, else $\phi \in]-\pi,0[$, $n_w = -1$. Here we have two different chiralities according to the phase. And thus, different topological insulators according to the Chern number (fig.8).

During a topological phase transition at one Dirac point, the Chern number varies of ± 1, whereas the second Dirac point is not affected.
We can see that in the evolution of Berry curvature according the evolution of the parameters. In fact, each peak has a contribution to the winding number $\pm\frac{1}{2}$, according its direction. In the case where the time reversal symmetry is conserved, the curvature is odd : $\Omega(\vec{k}) = -\Omega(\vec{k})$, and thus $n_w = 0$. When this symmetry is broken, the peaks are in the same direction, and have an identical contribution (fig.9). To be sure that the low energy study is pertinent, we have plotted the Berry curvature in the continuous limit as in the figure 10. There is no differences between the two plots, so our approximation is correct, because the only contact points are the Dirac points, but if we imagine a third band with a contact point somewhere else, we must to stay in the continuous limit. It is one of the purpose of the following part.

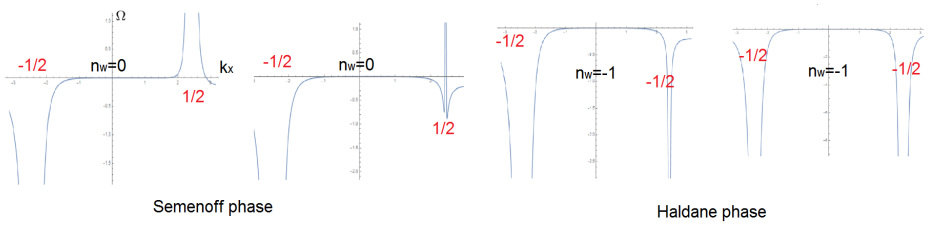

Figure 9: Berry curvatures of each phase in the low energy development, the variation of the winding number depends on the direction of the singularity in the Dirac point.

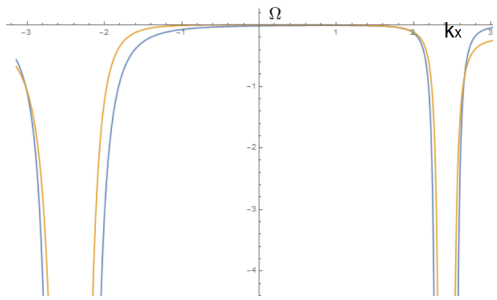

Figure 10: A good concordance between the continous model and the low energy approximation, in blue the low energy plot, in yellow the continuous one.

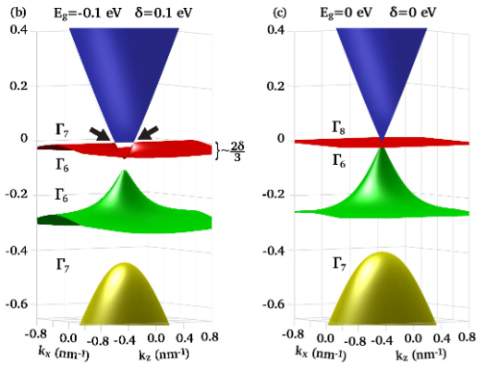

Figure 11: An example of three-band material : Cd_3As_2, with Dirac cones and a flat band. We observe a band connected to another one by two Dirac cones (left), and when we distort the structure, the red band becomes flat and cut the Dirac cone betweem the blue and the green ones.

3 Three-band model

As we can see in the figure 11, the Cd_3As_2 is a three dimensionnal material which has a particular band structure. The flat band (in red) formed two linear contacts with the blue one. As we are in 3D, these are Weyl-fermions. However, a continous deformation of parameter yields to a Dirac cone in Γ point : two linear bands (blue and green) cut by one flat band. A motivation here is to understand what is probed experimentally : low-energy Weyl points or linear blue-green dispersion. The two non-flat bands don't seem to be topological. In this study, we want to understand this situation in a simpler 2D model with additional flat band. In order to study the three-dimensionnal case, with Weyl fermions, we start an easier study in two dimensions, but with three bands (as in three dimensions). The third band has certainly an important role due to correlation.

3.1 A reference lattice : Kagomé

The Kagomé lattice (fig.12) is defined by three vectors connecting the inequivalent sites A, B and C : $\vec{a_1} = \frac{1}{2}\vec{e_x} - \frac{\sqrt{3}}{2}\vec{e_y}$, $\vec{a_2} = -\frac{1}{2}\vec{e_x} - \frac{\sqrt{3}}{2}\vec{e_y}$ and $\vec{a_3} = \vec{e_x}$. Each of the sublattices (A, B and C) is a triangular Bravais lattice, such that the reciprocal lattice is identical to that of graphene.

The Hamiltonian of a such system is given under in matrix form by :

$$H_0 = \begin{pmatrix} 0 & 2t\cos k_2 & 2t\cos k_1 \\ 2t\cos k_2 & 0 & 2t\cos k_3 \\ 2t\cos k_1 & 2t\cos k_3 & 0 \end{pmatrix}, \tag{17}$$

where we have used the notation $k_i = \vec{k}.\vec{a_i}$.

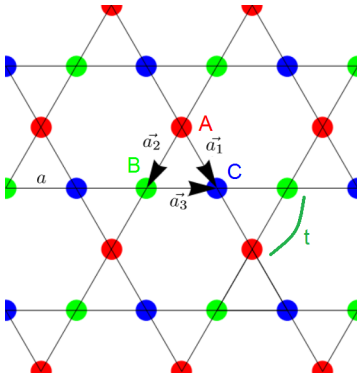

Figure 12: Kagomé lattice, defined by the vectors $\vec{a_1}, \vec{a_2}$ and $\vec{a_3}$.

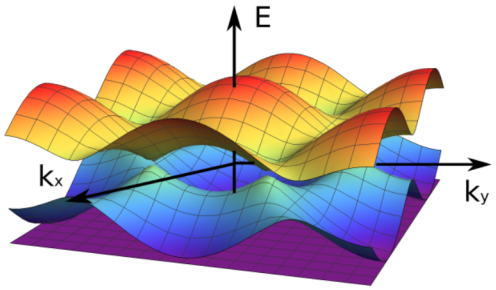

Figure 13: The Kagomé spectrum, three bands whose one is flat as in Cd_3As_2, and the two others are Dirac-like.

This Hamiltonian gives the following spectrum, normalized in the hopping term t (fig.13) :

- $E_0 = -2$,
- $E_\pm = 1 \pm 2\sqrt{4(\cos^2 k_1 + \cos^2 k_2 + \cos^2 k_3) - 3}$.

We can observe that one of these bands is flat, although it is not decorrelated from the others. The two others are very similar to the bands of graphene, and meeting in two inequivalents points $\vec{K} = \xi\frac{2\pi}{3}\vec{a_3}$, forming Dirac cones (seen thanks to a linearisation around these points), while the flat band touches the middle band at the Γ point.

3.2 Band characterization

As in the two-band case, we are looking for a characterization of the bands by the Berry curvature (Eq.5). The problem here is the following : we have several contact points. Firstly, between two Dirac-like bands in Dirac points, and secondly, between the lowest Dirac-like band and the flat one in Γ point. To compute a Chern number, we have to separate these bands, i.e. to open a gap as in two-band models.

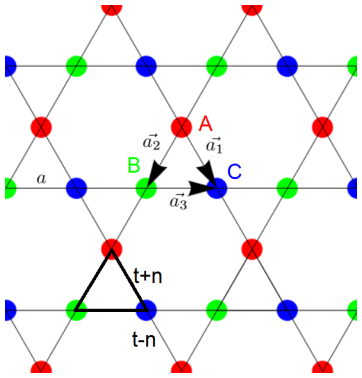

Figure 14: Semenoff-like interaction for Kagomé lattice.

3.2.1 Gapping processes

To open a gap or move the flat band, we are looking for a generalisation of the two-band case, similarly to Semenoff and Haldane's ideas.
There is another mathematical way to do this : consider a prediagonalisation according to the flat state (see appendix), which can also be helpful to compute eigenstates and Berry phase or Chern number.

In a first step I propose to open a Semenoff-type gap, with a little difference here : instead of adding a onsite potential, I propose to dimerize the links by using different hopping parameters. On the up-triangles, the hopping is $t+n$, while I choose $t-n$ on the down-triangles (fig.14).
Such a configuration adds the following Hamiltonian to H_0 :

$$H_s = \begin{pmatrix} 0 & 2ni\sin k_2 & 2ni\sin k_1 \\ -2ni\sin k_2 & 0 & 2ni\sin k_3 \\ -2ni\sin k_1 & -2ni\sin k_3 & \end{pmatrix}, \tag{18}$$

which effectively gives rise to an opening of the gap between the two non-flat bands, as seen in figure 15.

From a Haldane point of view, we consider in the same way the interaction to the second nearest neighbours, but in this case, only imaginary $i\lambda$ in a direction, and $-i\lambda$ in the other, as in figure 16. To the Hamiltonian H_0, we thus add :

$$H_h = 2i\lambda \begin{pmatrix} 0 & \cos(k_1+k_3) & \cos(k_3-k_2) \\ -\cos(k_1+k_3) & 0 & \cos(k_2+k_1) \\ -\cos(k_3-k_2) & -\cos(k_2+k_1) & 0 \end{pmatrix}, \tag{19}$$

which gives rise to a gap(fig.17), but also to a displacement of the flat band, which permits to have three isolated bands for which we could compute the Chern numbers.

As in the two bands models, such perturbations give certainly rise to topological phase transition according to n and λ. It is the purpose of the following section.

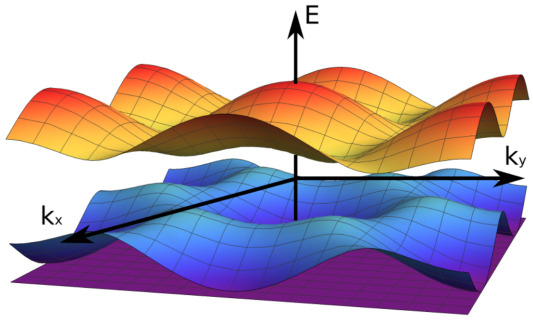

Figure 15: Spectrum of the dimerized Kagomé lattice which opens a gap between the Dirac bands.

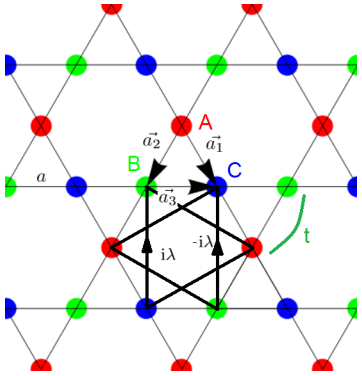

Figure 16: Haldane-like interaction for Kagomé lattice.

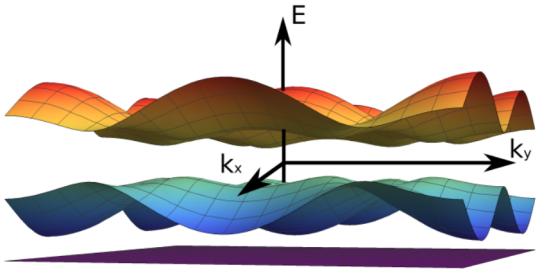

Figure 17: Spectrum of the Haldane-like Kagomé lattice which gives three isolated bands.

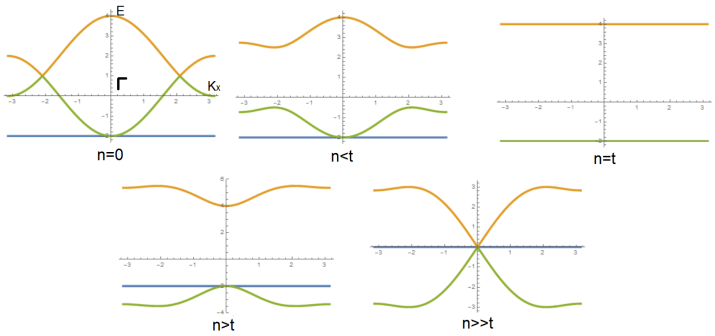

Figure 18: Several bands structures according to n in the k_x direction.

3.2.2 Topological phase transition

A simple study is to find the gap closure according to n and λ. Indeed, as in the two-band model, we can define a border where the gap is closed by compensation between the two terms : $n = 4\sqrt{3}|\lambda|$, and define a phase where the "Semenoff" term is dominant in front of the "Haldane" term for $n > 4\sqrt{3}|\lambda|$, and inversely in the other case. This can be seen in the band structure, and similarly, we can expect that crossing this border is accompanied by a change in Chern numbers of the Dirac bands in +1 for one band, and -1 for the second, and an invariance for the flat band Chern number. We can question the role of the flat band here, and we therefore study also these two phases to probe if there are others topological phase transitions between the flat band and the lowest band due to their contact in Γ point.
In order to probe the phase diagram, it consider different cases : firstly when λ is null and modifying n, then inversely.

In the Semenoff-like phase

The eigenvalues of the Hamiltonian $H_0 + H_s$ are :

- $E_0 = -2t$,
- $E_\pm = t \pm \sqrt{4(t^2 A_{\vec{k}} - n^2 B_{\vec{k}}) - 3t^2}$,

where we have written $A_{\vec{k}} = \cos^2 k_1 + \cos^2 k_2 + \cos^2 k_3$ and $B_{\vec{k}} = \sin^2 k_1 + \sin^2 k_2 + \sin^2 k_3$. The evolution of the band structure is shown in 18 as a function of n.

When $n < t$, the gap is opened between the two bands until $n = t$. In this particular case, we have three flat bands, one at $E = 4t$, and a twofold degenerate one at $E = -2t$. This corresponds to the particular case where we have isolated triangles as in figure 19.
We can easily compute the eigenvalues and the eigenstates of a such system, by the Hamiltonian for a single triangle :

$$H_{triangle} = \begin{pmatrix} 0 & t & t \\ t & 0 & t \\ t & t & 0 \end{pmatrix}, \tag{20}$$

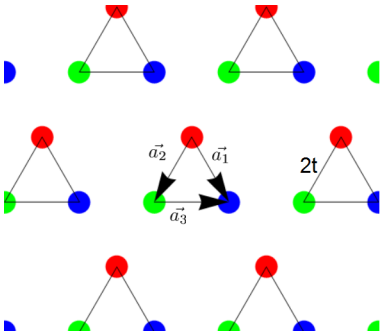

Figure 19: Isolated triangles corresponding to the flat bands spectrum.

which can be written thanks to the rotation matrices $R_3 = \begin{pmatrix} 0 & 1 & 0 \\ 0 & 0 & 1 \\ 1 & 0 & 0 \end{pmatrix}$, whose eigenvalues are $e^{\frac{i2\pi n}{3}}$, with n=0,1,2, and thus the eigenvalues of $H_{triangle} = t(R_3 + R_3^\dagger)$ are $E_n = 2t\cos\frac{2\pi n}{3}$.

If $n > t$, we can see that the lower Dirac-like band and the flat one are inversed : in general, this can be translated by a topological phase transition. In order to show it, we have to compute the Chern number. And we have the extremal case, where $n \gg t$, where we have a Dirac cone at the Γ point cut by the flat band. This situation is thus similar to the deformed (3D) band structure of Cd_3As_2 mentionned at the beginning of this section. I would like to stress that this cone is unexpected in a two-band model because of time reversal symmetry that precludes a Dirac point at Γ point : what is the nature of the fermion ? We can answer to this question studying the Chern number and Berry curvature. The main issue here is that we have two bands in contact, and so we are unable to compute the Berry curvature, for non isolated band. However, we are able to have separated bands with the Haldane-like perturbation.

In the Haldane-like phase

The eigenvalues of the Hamiltonian $H_0 + H_h$ are :

- $E_0 = E_p(\lambda) = -2 - 3|\lambda|$,
- $E_\pm = \frac{-E_p(\lambda)}{2} \pm \frac{1}{2}\sqrt{4(t^2 A_{\vec{k}} + \lambda^2 C_{\vec{k}}) - 3E_p(\lambda)}$,

where we have used $A_{\vec{k}}$ as in the preceeding case, and $C_{\vec{k}} = \cos^2(k_1 + k_2) + \cos^2(k_3 - k_2) + \cos^2(k_1 + k_3)$.
As in the previous paragraph, we are probing this region of the phase diagram at $n = 0$, modifying λ. The band structure according to n is shown in figure 20.
We can see that the gap is opened when $\lambda > 0$, and the flat band is moving. We are thus able to decouple the bands. There is an inversion in the curvature of the orange and green bands around $\lambda = 0.4$, which arrives to the case $\lambda \gg t$. Here it is more difficult to talk about transition but we can assume it. Less work has been done here, due to a lack of time.

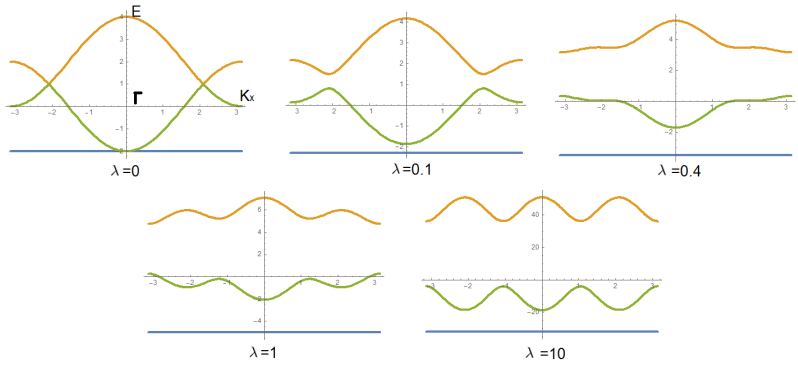

Figure 20: Several bands structures according to $\frac{\lambda}{t}$ in the k_x direction.

Finally, we can make the following hypothetical phase diagram obtained probing the entire space (n,λ), where we can assume some changement in Chern numbers, and be more prudent for others (fig.21). The main hypothesis here are the changement in the band structure as in figure 18 and 20. The red lines correspond hypothetically to the points (n,λ) where the three bands are flat. The green lines corresponds to the points where the upper bands become sinusoidal.
As we refer to the two-band model, the black border correspond to a change of Chern number for the Dirac-like bands of ± 1. The second idea here, is the possibility of change of Chern number with the flat band. The main hypothesis here is only the two lowest bands are in contact at Γ point, so maybe only between them is a change of Chern number. We expect that, because these two bands are inverted for $n = t$.
The variation according to λ is only hypothetical, and we need more work to check it.

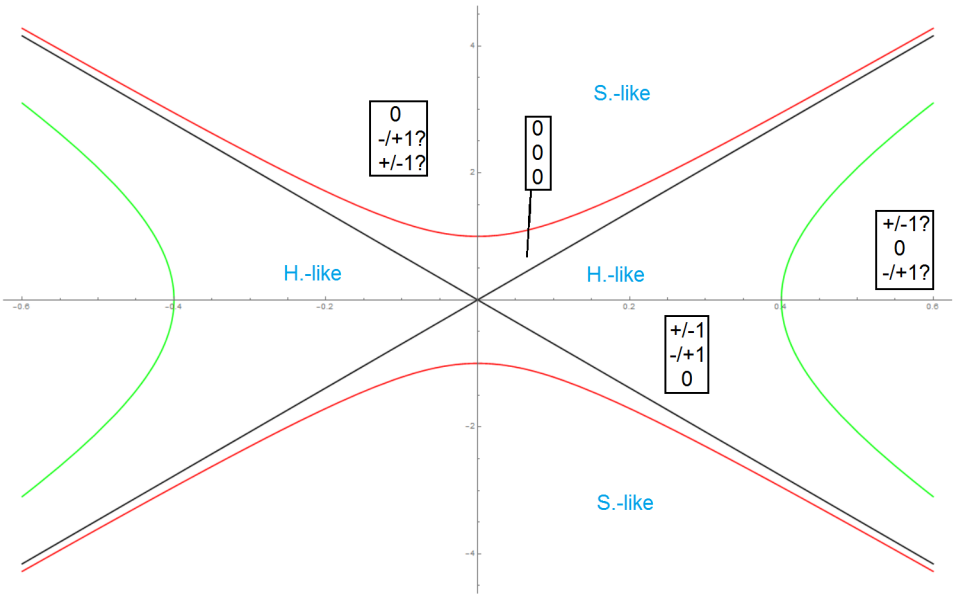

Figure 21: Hypothetical phase diagram of the Kagome lattice : the red and green curves are hypothetical, but could traduce a change of Chern number between the two lowest bands. We have opposite Chern numbers by symmetry. In each frame, the upper number corresponds to the upper band one, the second to the lower Dirac band, and the last one to the flat band.

4 Conclusion

The two-band model allows us to understand how to open a gap between bands and how to characterize the different phases according to the gap with topological numbers like Berry curvature. In a similar way, we have opened a gap in the Kagomé lattice, with Semenoff-like and Haldane-like models. We have a three-band phase diagram which is very close to the two bands one, and we expect the same evolution of Chern numbers for the Dirac-like bands according to the same borders.
Since we expect an impact due to the presence of the flat band, a good intuition is the evolution of the Chern numbers as in the last phase diagram, only between the bands in contact : flat and lowest Dirac-one.

5 Appendix

5.1 Dirac equation for graphene and Lorentz transformation

5.1.1 Dirac equation

The Hamiltonian describing relativistic particles must avoid negative probability density. To satisfy this, we need to have a linear equation at first order in the time derivative ∂_t. For Dirac, there is only the following ansatz which can satisfy this condition : $H = \beta mc^2 + \vec{\alpha}.\vec{p}$, such that : $E^2 = (\beta mc^2 + \vec{\alpha}.\vec{p})^2 = m^2c^4 + \vec{p}^2c^2$.
Hence we should have, $\beta^2 = \alpha_i^2 = \mathbb{1}$, $\{\beta, \alpha_i\} = 0$, $\{\alpha_i, \alpha_j\} = 2\delta_{ij} \Rightarrow$. This implies β, α_i are NxN matrices respecting the Clifford algebra* with N not necessarly the space dimension D.

In the graphene case, D=2, and we need to have three anticommuting matrices for β, α_1 and α_2. The Pauli matrices respect this algebra, thus we can take arbitrarly $\beta = \sigma_z$, $\alpha_1 = \sigma_x$ and $\alpha_2 = \sigma_y$.
And the Hamiltonian can be written, $H = \sigma_z mc^2 + c\vec{\sigma}.\vec{p}$, where $\vec{\sigma} = (\sigma_x, \sigma_y)$. If we take the Fermi velocity for c, we find a result developped previously, the massless Hamiltonian at low energy for graphene. This result can also be compared to the following one in the appendix 2.

*Clifford algebra :

- H hermitian $\Rightarrow$ α_i and β too.
- $\beta^2 = \alpha_i^2 = \mathbb{1} \Rightarrow$ unitary matrices with eigenvalues ± 1.
- Anticommutation of $\alpha_{i\neq}$, $det(\alpha_i\alpha_j) = (-1)^N det(\alpha_i\alpha_j) \Rightarrow$ N even.

5.1.2 Lorentz transformation

As for each relativistic system in a space-time of dimension D+1, we want to see the response to a Lorentz transformation L. Applying a such transformation to a scalar s, we obtain $s' = s$ and to a vector v^μ, $v'^\mu = \lambda^\mu_\nu v^\nu$ where λ describes the transformation.
A spinnor is transformed as follows : $\psi'(r', t') = S(L)\psi(r, t) = S(L)\psi(\lambda^{\mu\,-1}_\nu X^\nu)$,
with S(L) acting on the spinnor, but with some rules.
Considering the Dirac equation $H = \beta mc^2 + c\vec{\sigma}.\vec{p}$, applying it on the state ψ, we have the following equation $i\hbar(\partial_t + \alpha c\nabla)\psi = \beta mc^2\psi$ since $\vec{p}$ and $\vec{\sigma}$ commute.
Setting $\gamma^0 = \beta$ and $\gamma^i = \beta\alpha_i$, we can rewrite the last equation as $(p_\mu\gamma^\mu - mc)\psi(r, t) = 0$ which must be Lorentz invariant. That means $(p'_\mu\gamma^\mu - mc)\psi'(r', t') = 0$, and we obtain the following equation $[S^{-1}(L)\lambda^\nu_\mu p_\nu\gamma^\mu S(L) - mc]\psi(r, t) = 0$, we obtain finally $S^{-1}(L)\gamma^\mu S(L) = \lambda^\mu_\nu$ by comparison.

Parity and Time-reversal symmetry.

We define two Lorentz transformations, the parity P and the time riversal operator T in a space-time of dimension 4 :

$$P = \begin{pmatrix} 1 & 0 & 0 & 0 \\ 0 & -1 & 0 & 0 \\ 0 & 0 & -1 & 0 \\ 0 & 0 & 0 & -1 \end{pmatrix}, T = \begin{pmatrix} -1 & 0 & 0 & 0 \\ 0 & 1 & 0 & 0 \\ 0 & 0 & 1 & 0 \\ 0 & 0 & 0 & 1 \end{pmatrix}$$

In the example of the 2D graphene, $\gamma^0 = \sigma_z$, $\gamma^i = \sigma_z\sigma_i$, which implies :
for the parity transformation, $S = \sigma_z P$, and for the time reversal transformation, $S = \sigma_y CT$, where C is the complex conjugation operator.

5.2 Eigenstates and eigenenergies in a two bands model

To simplify our study, we can exhibit a good basis for hermitian matrices of $M_2(\mathbb{C})$, which can permit us to compute easily the eigenvalues and the eigenstates of the different Hamiltonians.
We consider the family $(\mathbb{1}, \sigma_x, \sigma_y, \sigma_z)$, which is a basis for the set of matrices considered in terms of the Pauli matrices.

$$\sigma_x = \begin{pmatrix} 0 & 1 \\ 1 & 0 \end{pmatrix}, \sigma_y = \begin{pmatrix} 0 & -i \\ i & 0 \end{pmatrix}, \sigma_z = \begin{pmatrix} 1 & 0 \\ 0 & -1 \end{pmatrix}$$

We can thus describe an Hamiltonian in 2D :
$H = h_0\mathbb{1} + h_1\sigma_x + h_2\sigma_y + h_3\sigma_z = h_0\mathbb{1} + \vec{h}.\vec{\sigma}$.
From this, if we rewrite the Hamiltonian in a matrix form :

$$H = \begin{pmatrix} h_0 + h_z & h_x - ih_y \\ h_x + ih_y & h_0 - h_z \end{pmatrix}$$

The spectrum can be written : $\epsilon = h_0 \pm |h|$
About the eigenstates, we have to solve the following equation : $\vec{h}.\vec{\sigma}|\phi^{\pm}\rangle = \pm|h||\phi^{\pm}\rangle$
where $\pm$ denotes the conduction (-) or the valence (+) band.
Such equation has for solution :

$$|\phi^{\pm}\rangle = \frac{1}{\sqrt{2}} \begin{pmatrix} \sqrt{1 + \frac{\pm h_z}{|h|}} \\ \pm\sqrt{1 - \frac{\pm h_z}{|h|}}\, e^{i\theta} \end{pmatrix}$$

where $\tan\theta = \frac{h_y}{h_x}$.
We can also define $\frac{\vec{h}.\vec{\sigma}}{|h|}$ as the helicity operator, with eigenvalues $\eta = \pm$, which defines the chirality.
For example, in the graphene case, according to the spinors associated, $\pm$ defines the polarization of the isospin according to its direction : For +, it is the parallel case and for - it is the antiparallel case.
Finally, we have $\lambda = \xi\eta$, where λ defines the band (conduction or valence) and ξ the valley (the site of the Dirac cone).
And we can resume the chirality on the figure 22.

5.3 Berry phase, Berry curvature and Chern number

We have periodic boundary conditions for k_x and k_y in the graphene. So we can reduce the study only to the first Brillouin zone, because the rest of reciprocal space

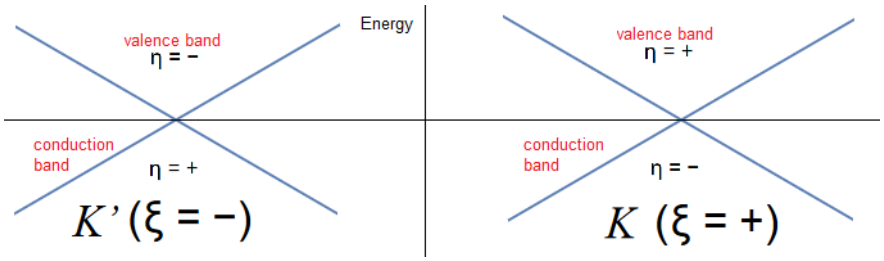

Figure 22: Chirality of the graphene.

is just replica of the first Brillouin zone.
In fact, this is topologically equivalent to say that we can compare this first Brillouin zone to a torus. A such topology is defined by some concepts : Berry phase, Berry curvature, ... which are extremely sensitive to the singularities in the wavefunctions. These concepts give informations about the quasiparticle considered, beyond the only spectrum.

5.3.1 Berry phase

We assume a ground state $|\psi(\alpha)\rangle$ non degenerated, which satisfies the Schrödinger equation :

$$H(\alpha)|\psi(\alpha)\rangle = E(\alpha)|\psi(\alpha)\rangle,$$

where α is a parameter, to which we consider an adiabatic evolution (we are in a spectrum of frequencies much bigger than the gap energy) between α_1 and α_2.
According to the time dependent Schrödinger equation we obtain a dephasing :
$e^{-i\phi_{12}} = \langle\psi(\alpha_2)|\psi(\alpha_1)\rangle$, from which we can write :
$\phi_{12} = -\Im(\ln(\langle\psi(\alpha_2)|\psi(\alpha_1)\rangle))[2\pi]$.
If we consider a closed path between four points : $\alpha_1, \alpha_2, \alpha_3$ and α_4, we obtain a total dephasing of $\gamma = \phi_{12} + \phi_{23} + \phi_{34} + \phi_{41}$. This dephasing is called Berry phase, and seems to be dependent of the evolution of α.
In the continuum limit,
$e^{-i\Delta\phi} =< \psi(\alpha)|\psi(\alpha + \Delta\alpha) >$,
which gives at first order,
$-id\phi = \langle\psi(\alpha)|\nabla_\alpha\psi(\alpha)\rangle d\alpha$, from that, we derive the Berry connexion $\vec{A(\alpha)} = i\langle\psi(\alpha)|\nabla_\alpha\psi(\alpha)\rangle$.
The Berry phase is thus written : $\gamma = \oint \vec{A(\alpha)}.\vec{d\alpha}$. A such path can be the Bloch sphere for the spin or a Dirac cone.

5.3.2 Berry curvature, Chern number and winding number

By the Stokes theorem we can rewrite :
$\gamma = \iint \vec{\Omega}.\vec{dS}$, where $\vec{\Omega}$ is the Berry curvature : $\Omega_{\mu\nu} = \nabla_\alpha\langle\psi(\alpha)| \wedge \nabla_\alpha|\psi(\alpha)\rangle$.
We can directly see that the Berry phase is parallel transport : the angle between the initial state and the final state. The Berry phase teaches us about the chirality of the system.
We have introduced a vector $\vec{h}$ which describes the hamiltonian with the Pauli matrices. This vector is a function of the momentum $\vec{k}$, it is a mapping between the Bloch sphere

(S^2) and the Brillouin zone (T^2). We understand that $\vec{k}$ is in fact a parameter moving in the BZ induces a parallel transport in the spinor !
We recall the expression of the spinors (+ valence band, - conduction band) :

$$|\phi^{\pm}\rangle = \frac{1}{\sqrt{2}} \begin{pmatrix} \sqrt{1 + \frac{\pm h_z}{|h|}} \\ \pm\sqrt{1 - \frac{\pm h_z}{|h|}} e^{i\theta} \end{pmatrix},$$

these spinors can be rewritten in terms of the angles on the Bloch sphere using $\frac{\vec{h}}{|h|} = (\sin\theta\cos\phi, \sin\theta\sin\phi, \cos\theta)$:

$$|\phi^{+}\rangle = \begin{pmatrix} \cos\frac{\theta}{2} e^{i\phi} \\ \sin\frac{\theta}{2} \end{pmatrix}, \; |\phi^{-}\rangle = \begin{pmatrix} \sin\frac{\theta}{2} e^{-i\phi} \\ -\cos\frac{\theta}{2} \end{pmatrix}.$$

Hence, computing the Berry connexion (in two dimensions, with real components for the eigenstates) : $A^- = \nabla\phi \sin^2\frac{\theta}{2}$ and $A^+ = -\nabla\phi\cos^2\frac{\theta}{2}$,
and the Berry curvature (in two dimensions, with real components for the eigenstates) : $\Omega^- = \frac{1}{2}\sin\theta(\partial_{k_x}\theta\partial_{k_y}\phi - \partial_{k_y}\theta\partial_{k_x}\phi) = -\Omega^+$.
In fact, in two-bands model, we are able to rewrite the Berry curvature with the help of $\vec{h}$: $\Omega^{\alpha}_{\vec{k}} = \frac{\alpha}{4\pi}\frac{1}{|\vec{h}|^3}\vec{h}.(\partial_{k_x}\vec{h}\wedge\partial_{k_y}\vec{h})$. There is also another way to write it, in a general two-dimensionnal case, for two or three bands model : $\Omega_{\vec{k}} = \langle\partial_{k_x}\psi|\partial_{k_y}\psi\rangle - \langle\partial_{k_y}\psi|\partial_{k_x}\psi\rangle$, where ψ is the eigenstate.

The Chern number permits to characterize some topological phases, where there is no order parameter. In fact, it is an easier way to characterize instead of the Berry curvature. Indeed, this number is computed from the Berry curvature. We are only interested in the conduction band, which describes the winding number n_w, the number of winding around the Bloch sphere, and thus the dynamic of the system.

$$C^- = \frac{1}{4\pi}\int_{BZ} d^2k \sin\theta(\partial_{k_x}\theta\partial_{k_y}\phi - \partial_{k_y}\theta\partial_{k_x}\phi).$$

5.4 Eigenstates and eigenenergies in a three bands model

Similarly, we are looking for a friendly basis to compute the eigenstates and eigenenergies of a three bands model. As described in the previous annex, we want to define a vector $\vec{h}$ to describe the Hamiltonian. We are looking for a basis of Pauli-like matrices, which can generate the hermitian matrices of $M_3(\mathbb{C})$.
In a three band model, the Hamiltonian in second quantification can be written :

$$\begin{pmatrix} h_{11} & h_{12} & h_{13} \\ h_{12}^* & h_{22} & h_{23} \\ h_{13}^* & h_{23}^* & h_{33} \end{pmatrix}$$

Thus, we define 9 matrices $\sigma_x^{1,2,3}$, $\sigma_y^{1,2,3}$ and $\sigma_z^{1,2,3}$, such that :

$$\sigma_x^1 = \begin{pmatrix} 0 & 1 & 0 \\ 1 & 0 & 0 \\ 0 & 0 & 0 \end{pmatrix}, \; \sigma_x^2 = \begin{pmatrix} 0 & 0 & 1 \\ 0 & 0 & 0 \\ 1 & 0 & 0 \end{pmatrix}, \; \sigma_x^3 = \begin{pmatrix} 0 & 0 & 0 \\ 0 & 0 & 1 \\ 0 & 1 & 0 \end{pmatrix}$$

$$\sigma_y^1 = \begin{pmatrix} 0 & -i & 0 \\ i & 0 & 0 \\ 0 & 0 & 0 \end{pmatrix}, \; \sigma_y^2 = \begin{pmatrix} 0 & 0 & i \\ 0 & 0 & 0 \\ -i & 0 & 0 \end{pmatrix}, \; \sigma_y^3 = \begin{pmatrix} 0 & 0 & 0 \\ 0 & 0 & -i \\ 0 & i & 0 \end{pmatrix}$$

$\sigma_z^1 = \begin{pmatrix} 1 & 0 & 0 \\ 0 & 0 & 0 \\ 0 & 0 & 0 \end{pmatrix}$, $\sigma_z^2 = \begin{pmatrix} 0 & 0 & 0 \\ 0 & 1 & 0 \\ 0 & 0 & 0 \end{pmatrix}$, $\sigma_z^3 = \begin{pmatrix} 0 & 0 & 0 \\ 0 & 0 & 0 \\ 0 & 0 & 1 \end{pmatrix}$

The σ_z matrices commute because they respect the Cartan algebra : we need only two matrices, not three, because we refind the identity by combination. Hence we can write : $H = \vec{h}.\vec{\sigma}$, with $\vec{h} = (h_{x1}, h_{x2}, h_{x3}, h_{y1}, h_{y2}, h_{y3}, E_1, E_2, E_3)$ and $\vec{\sigma} = (\sigma_x^1, \sigma_x^2, \sigma_x^3, \sigma_y^1, \sigma_y^2, \sigma_y^3, \sigma_z^1, \sigma_z^2, \sigma_z^3)$, and we can now compute the eigenvalues (too complex to be written here).
Moreover, we have the following commutation and anticommutation relations for the matrices σ_x and σ_y :
$[\sigma_x^i, \sigma_x^j] = i\epsilon^{ijk}\sigma_y^k$, $[\sigma_y^i, \sigma_y^j] = -i\epsilon^{ijk}\sigma_y^k$, $[\sigma_x^i, \sigma_y^j] = i\epsilon^{ijk}\sigma_x^k$,
$\{\sigma_x^i, \sigma_x^j\} = \sigma_x^k$, $\{\sigma_y^i, \sigma_y^j\} = -\sigma_x^k$, $\{\sigma_x^i, \sigma_j^j\} = \epsilon^{ijk}\sigma_y^k$.

5.5 Prediagonalisation and opening of gap

5.5.1 Prediagonalisation transformation

In a two bands model, it is almost trivial to see how we can open a gap or move bands. For a three bands model, it is more difficult because we have couplings between each band. Since we are interested in the flat band, the idea of the following paragraphs is to do a prediagonalisation of the Hamiltonian, to separate the flat band. What is a such transformation ? Here, it is presented a mathematical solution.

We assume we know the eigenstate $\frac{1}{\sqrt{a^2+b^2+c^2}} \begin{pmatrix} a \\ b \\ c \end{pmatrix}$ of the flat band, easier to be found, since the eigenvalue is a constant λ. We are looking for a trans formation U unitary, it means $U^\dagger U = \mathbb{1}$. So,

$$U = \frac{1}{\sqrt{a^2+b^2+c^2}} \begin{pmatrix} a & \sqrt{b^2+c^2} & 0 \\ b & \frac{-ab}{\sqrt{b^2+c^2}} & -c\frac{\sqrt{a^2+b^2+c^2}}{\sqrt{b^2+c^2}} \\ c & \frac{-ac}{\sqrt{b^2+c^2}} & b\frac{\sqrt{a^2+b^2+c^2}}{\sqrt{b^2+c^2}} \end{pmatrix}.$$

We obtain a new Hamiltonian, expressed in the prediagonalisation basis :

$$U^\dagger H U = H_{prediag} = \begin{pmatrix} \lambda & 0 & 0 \\ 0 & i(a,b,c,H) & j(a,b,c,H) \\ 0 & j^*(a,b,c,H) & k(a,b,c,H) \end{pmatrix},$$

where i,j and k define a two bands Hamiltonian H_2, which describes the two Dirac bands, and :
$i(a,b,c,H) = \frac{-2a(b^2+c^2)(bh_{x1}+ch_{x2})+(b^2+c^2)^2E_1+a^2(2bch_{x3}+b^2E_2+c^2E_3)}{(b^2+c^2)(a^2+b^2+c^2)}$,
$j(a,b,c,H) = \frac{b^3(h_{x2}+ih_{y2})-b^2(c(h_{x1}-ih_{y1})+a(h_{x3}-ih_{y3}))+c^2(-ch_{x1}+ah_{x3}+ich_{y1}+iah_{y3})+bc(c(h_{x2}+ih_{y2})+a(E_2-E_3)}{(b^2+c^2)\sqrt{a^2+b^2+c^2}}$
and,
$k(a,b,c,H) = \frac{-2bch_{x3}+c^2E_2+b^2E_3}{b^2+c^2}$.

5.5.2 Opening of gap

From $H_{prediag}$, we are able to separate the bands. Indeed, if we consider only H_2, describing the two Dirac bands as in the Kagomé case, we know already how to open

a gap. Indeed, we can apply a Semenoff perturbation, or a Haldane one, thanks to the matrice σ_z in two dimensions. To set this in the original basis, we express the matrix $\begin{pmatrix} 0 & 0 \\ 0 & \sigma_z \end{pmatrix}$, thanks to U by $G = U^\dagger \begin{pmatrix} 0 & 0 \\ 0 & \sigma_z \end{pmatrix} U$.
Finally,

$$G = \frac{1}{a^2+b^2+c^2} \begin{pmatrix} b^2+c^2 & -ab & -ac \\ -ab & a^2b^2 - c^2(a^2+b^2+c^2) & \frac{bc(2a^2+b^2+c^2)}{b^2+c^2} \\ -ac & \frac{bc(2a^2+b^2+c^2)}{b^2+c^2} & \frac{a^2b^2-b^2(a^2+b^2+c^2)}{b^2+c^2} \end{pmatrix}.$$

Similarly, to move the flat band in the prediagonalized basis, we use the matrix :

$$\begin{pmatrix} 1 & 0 & 0 \\ 0 & 0 & 0 \\ 0 & 0 & 0 \end{pmatrix}.$$

Applying U and $U^\dagger$, we have in the original basis :

$$D = \frac{1}{a^2+b^2+c^2} \begin{pmatrix} a^2 & ab & ac \\ ab & b^2 & bc \\ ac & bc & c^2 \end{pmatrix}.$$

Mathematically, we are now able to separate bands, and we can easily see that the Semenoff-like and Haldane-like perturbations are linear combinations of G and D.

5.5.3 Computing of topological numbers according to the transformation U

Since we have the following hamiltonian :

$$\begin{pmatrix} \lambda & 0 \\ 0 & H_{Dirac} \end{pmatrix}.$$

We can compute easily the Chern numbers of a such matrix, because the ones of H_{Dirac} is known. However, we have to compute it on the original basis. We denote by ψ' the eigenstates in the prediagonalised basis, and by ψ the ones in the original one, such that $\psi = U^\dagger \psi'$. From this, we can derive the Berry connexion :

$$A_{\vec{k}} = A'_{\vec{k}} + i\psi' U \nabla_{\vec{k}} U^\dagger \psi',$$

where $A'_{\vec{k}}$ denotes the Berry connexion in the prediagonalised basis.
In fact, we see that the flat band has an influence on the Berry connexions, and thus the Chern numbers of the Dirac-like bands only if there exists some singularities in its wavefunction, since U is made from it.

References

F.Rose, M.O. Goerbig and F. Piéchon, Phys. Rev. B **88** 125438 (2013)

L. Fu, C. L. Kane, and E. J. Mele, Phys. Rev. Lett. **98**, 106803 (2007)

J.N. Fuchs, F. Piéchon, M.O. Goerbig and G. Montambaux (2010)

A. Bernevig and T.L. Hughes, Topological insulators and topological sueprconductors (2013)

H.M. Guo and M. Franz, Phys. Rev. B **80**, 113102 (2009)

F.D.M. Haldane, Phys. Rev. Lett. **61**, 2015 (1988)

G.W. Semenoff, Phys. Lett. **53**, 2449 (1984)

C. Weeks and M. Franz, Phys. Rev. B **82**, 085310 (2010)